Comparison of Atmospheric Delay Statistics from Deep Space Network Arrays and nearby Site Test Interferometers

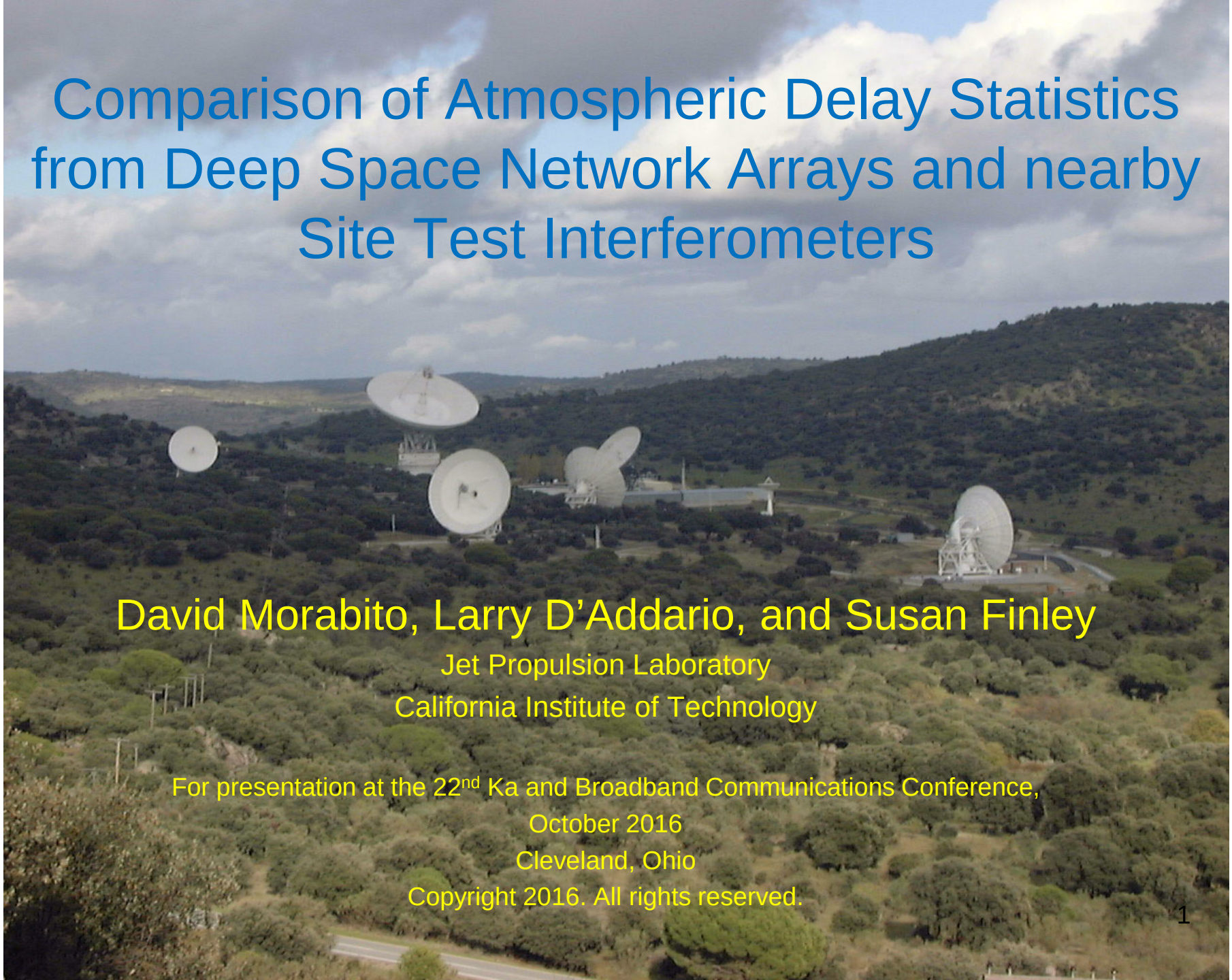

David Morabito, Larry D'Addario, and Susan Finley

Jet Propulsion Laboratory

California Institute of Technology

For presentation at the 22nd Ka and Broadband Communications Conference,

October 2016

Cleveland, Ohio

Copyright 2016. All rights reserved.

Scope

- **Background:** The DSN of the future will incorporate both uplink and downlink arraying. An important component of understanding the performance of arraying is the understanding of tropospheric propagation. The classical way of achieving this understanding is to use STIs.
- **Benefit to DSN**: The prediction of arraying loss magnitude and its dynamics
  - **Downlink Arrays** typically correct for the anomalies caused by tropospheric turbulence. However, the turbulence dynamics influence the design of the control loop. The characterization of a site by a STI will provide 1) information on the suitability of the site for arraying and 2) information for suitable design of the control loop.
  - **Uplink arrays** typically do not correct for turbulence effects, however, site characterization will allow the designer of the communications link to provide adequate margin to meet system requirements.
- **Infusion:** Statistics are annually updated into ITU data banks. It is planned to eventually incorporate the statistics into a new or existing DSN Telecommunications Link Design Handbook module. In addition to measured phase delay statistics, the procedures for calculating loss for a given array are documented.
- **This study:** Results of inter-comparisons of phase-delay data from a two-element array and nearby STI at Goldstone, California and Madrid, Spain.
- **NASA Activity:** NASA STI activity includes collaborations between JPL and GRC

The Global View

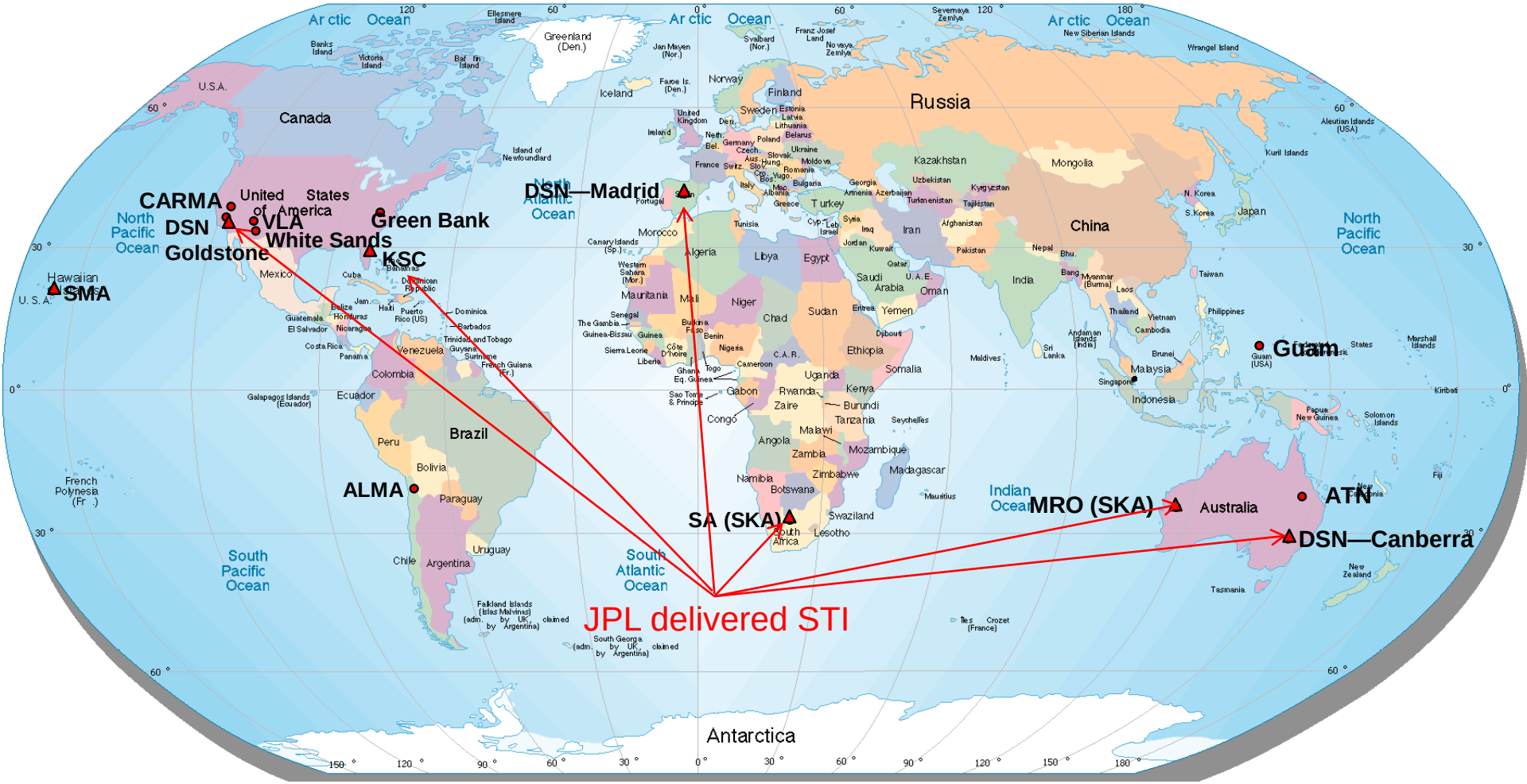

Theoretical Background

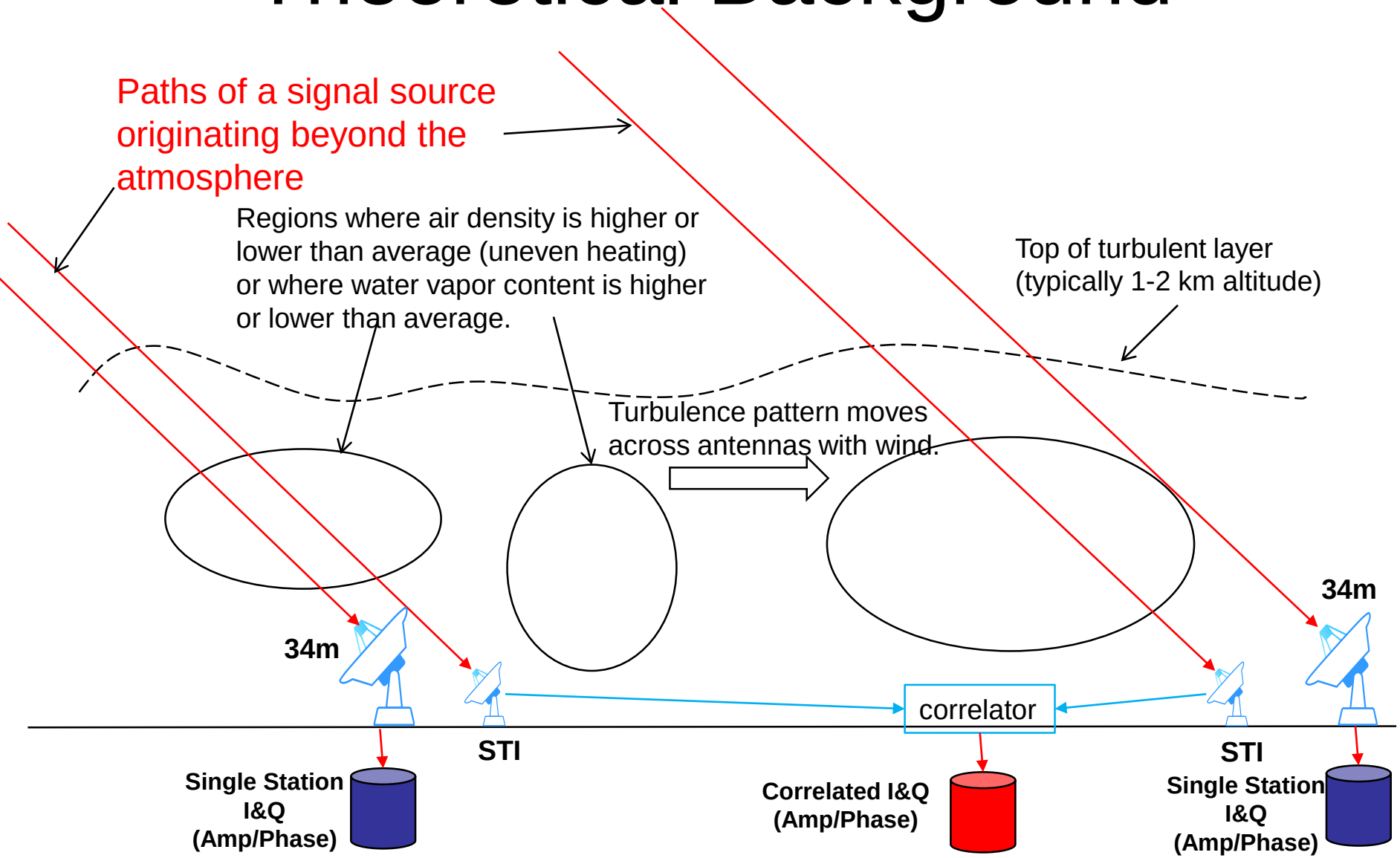

Apollo STI
(NASA JPL Equipment)

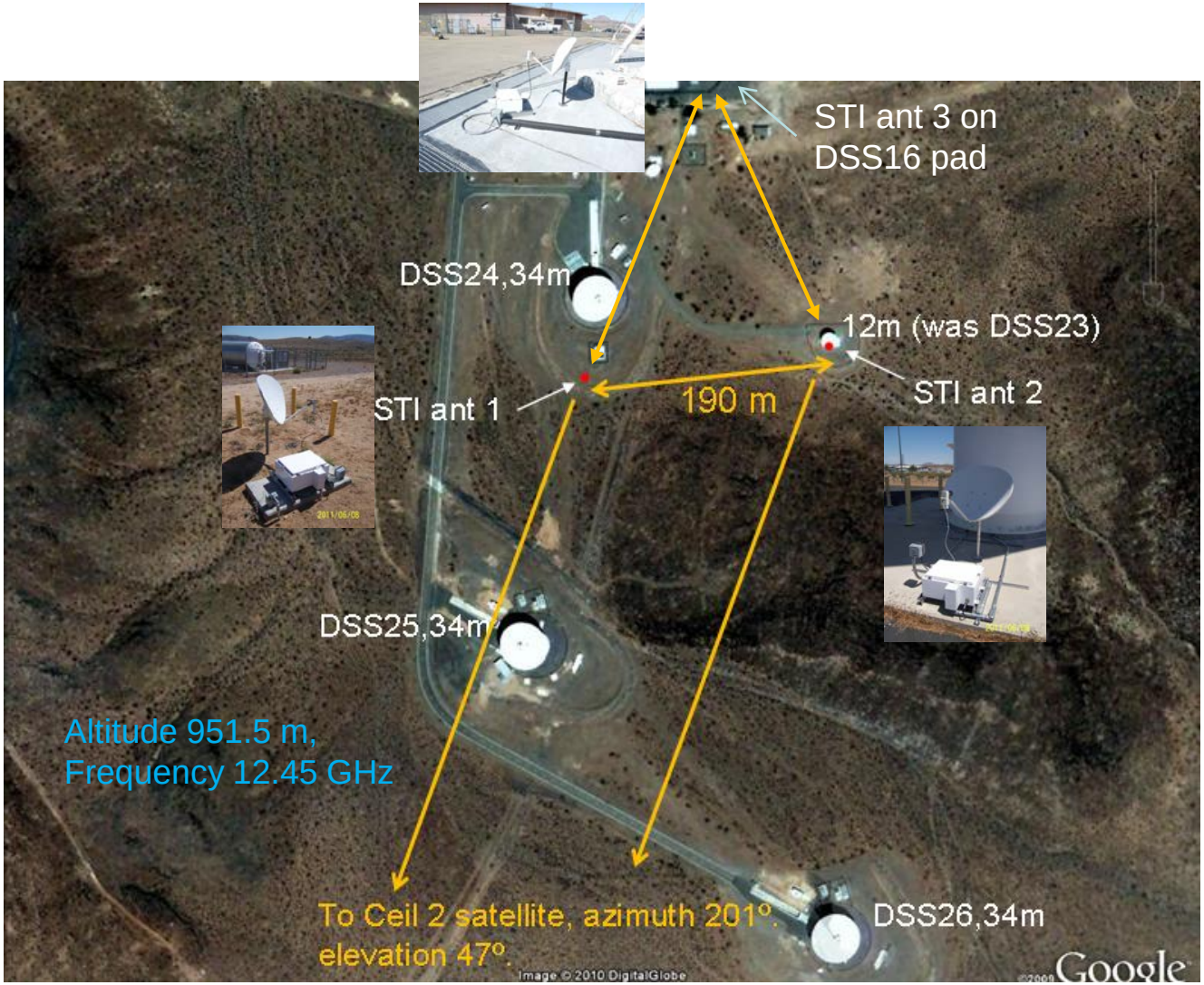

Array Demonstration - Kepler

- Array Data Processing
  - The carrier signal at 32.166 GHz emitted by the Kepler spacecraft was down-converted to baseband using in-phase (I) and quadrature-phase (Q) mixers driven by trajectory-based predictions of the carrier frequency.
  - The signal was low-pass filtered and digitally sampled at 1 ksps at each station of the two-element array.
  - The individual 1 ms samples from the recordings were pre-summed to output 0.1 s data points to match sampling time of the STI.
- STI Data Processing
  - The received signal from each STI element was downconverted to IF and sent to a central processing rack.
  - The IFs from each pair of elements were input to an IQ mixer board where the two signals were correlated and the resulting interferometric signal was captured in an output file.
  - During the post-processing, the phase time series estimated from the recorded I and Q samples was processed to remove cycle ambiguities, showing as well as short-term atmospheric fluctuations and thermal noise.
  - The slow changes were filtered over 10-minute blocks. The fitted model is subtracted from the phase data, and the resulting phase is dominated by short-term fluctuations due to atmosphere.
- Array and STI Phase Data Comparisons
  - To facilitate comparison of the STI measurements with those from the DSN array demonstration passes, the STI phases (or their statistics) are normalized or adjusted to conditions of the array by making adjustments for frequency, elevation angle, and baseline pair projection against signal source..

Table 1
Kepler Array Demonstration Passes

Pass ID	Date	DSS Stations	Data Span (UTC)
2014-316/317	Nov. 12-13, 2014	13/25 Goldstone	23:32 – 04:55
2015-192	July 11, 2015	25/26 Goldstone	00:50 – 01:00
2015-274	Oct. 01, 2015	25/26 Goldstone	21:54 – 23:55
2015-361	Dec. 27, 2015	25/26 Goldstone	01:52 – 05:00
2015-361	Dec. 27, 2015	54/55 Madrid	14:55 – 21:02

Examples of Turbulence-Induced delay differential (Goldstone)

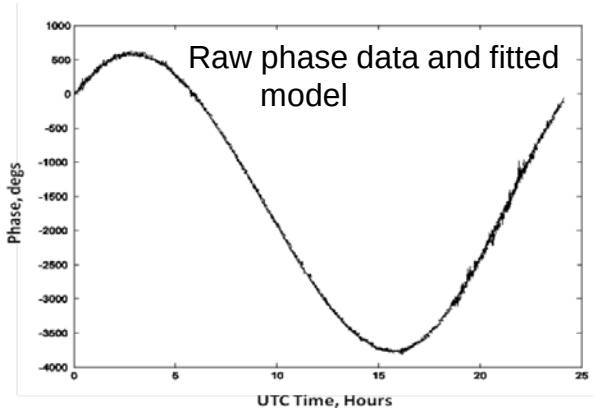

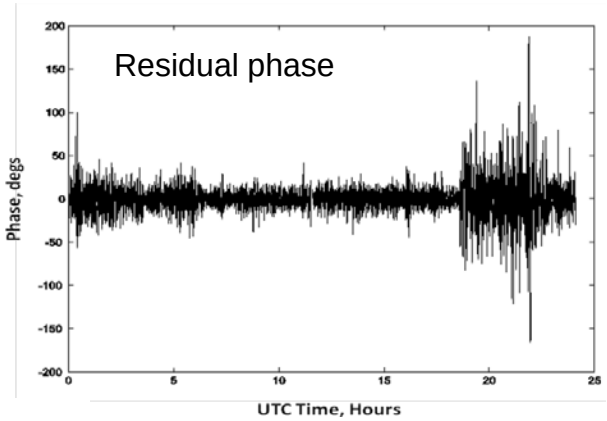

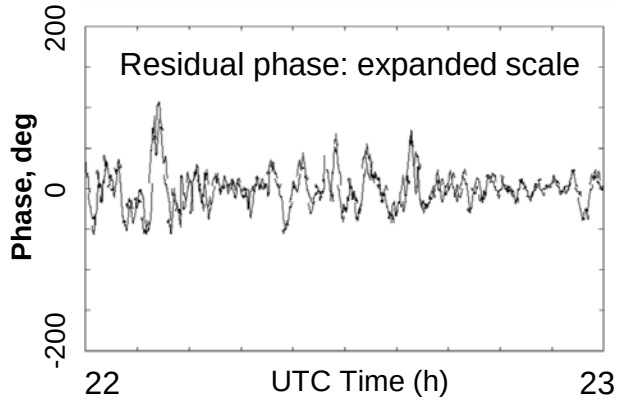

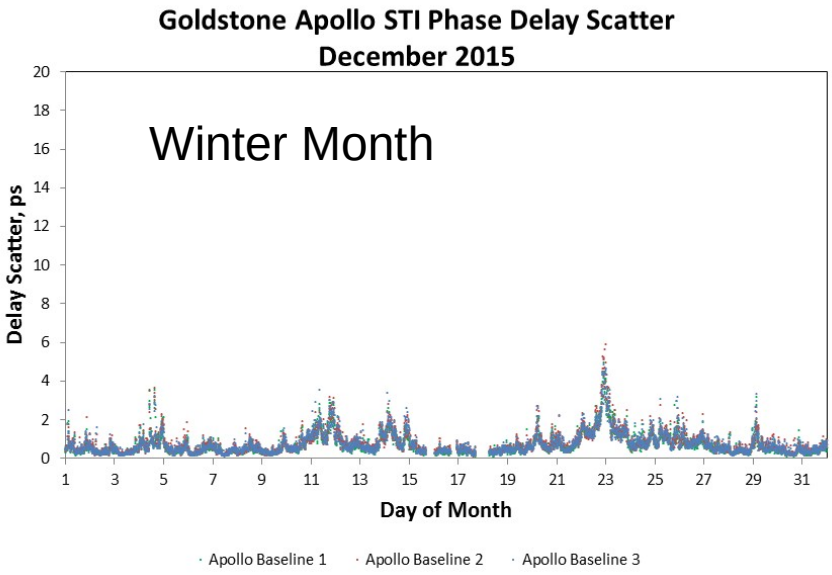

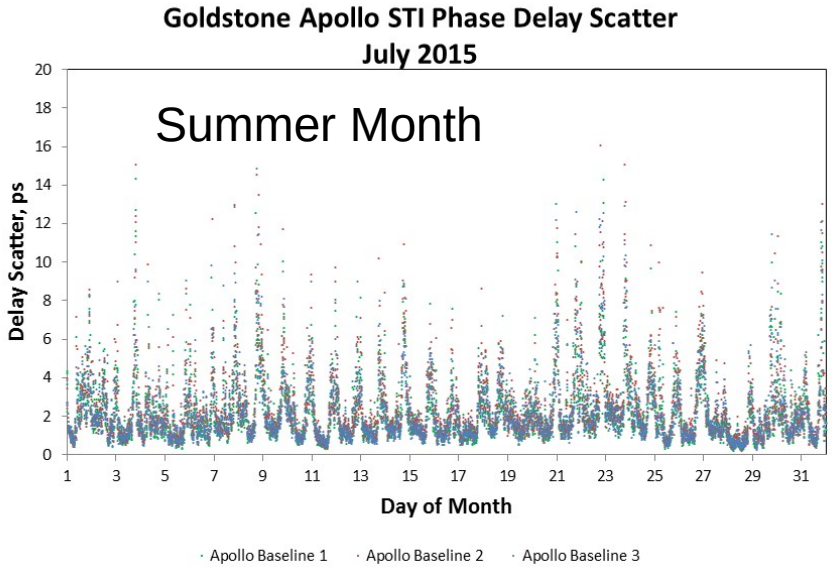

7

Site Test Interferometer Path Length Statistics

- Phase delay statistics can be converted to path length statistics
- Examples shown below for Goldstone STI with year-to-year variation (left) and monthly behavior (right)
- Reference: “Contributions to the Propagation Databanks: Path Length Turbulence Statistics for White Sands, NM; Goldstone, CA (Apollo Site); Canberra, AUST; Madrid, Spain; and Kennedy Space Center, Florida”, Document Number USSG3 3M-6 R00, ITU-R meeting in Geneva, June 2016.

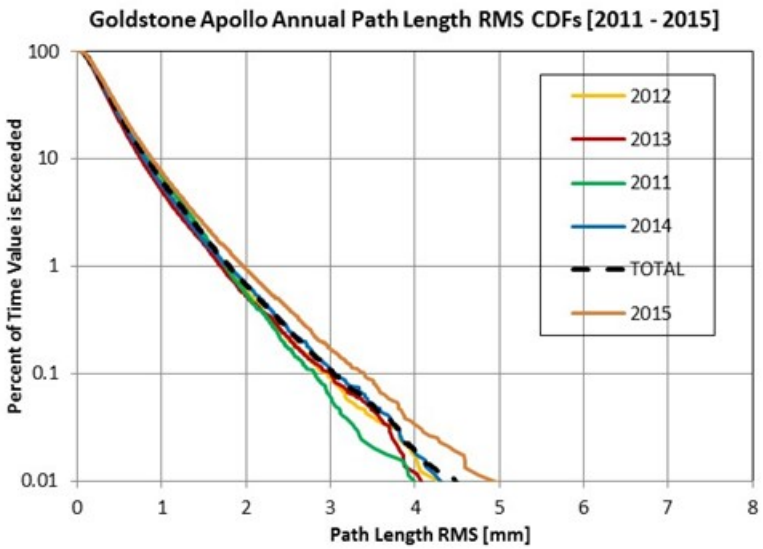

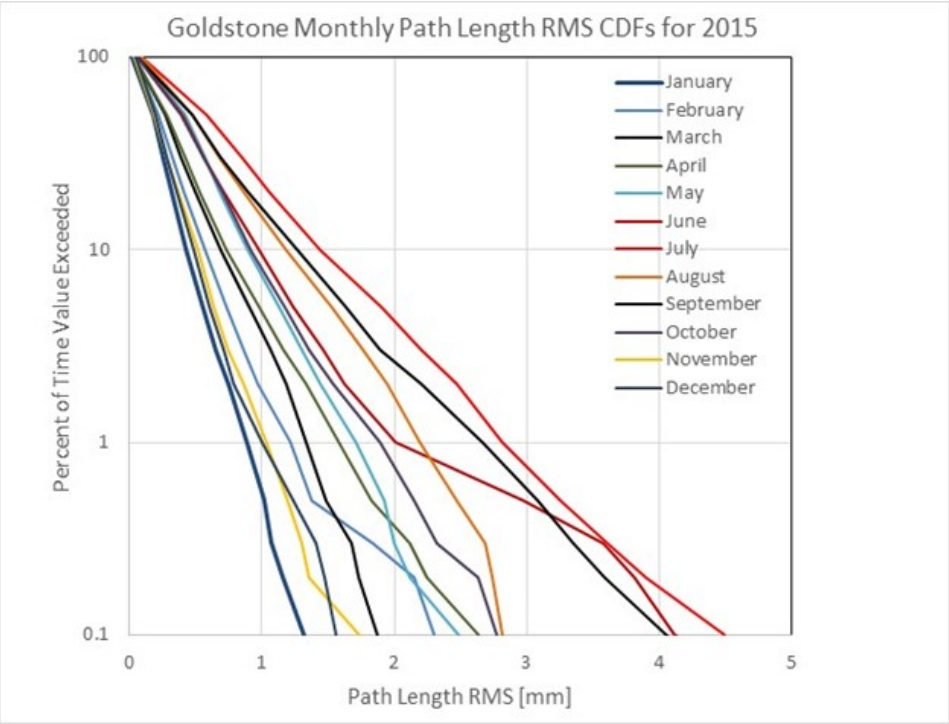

Use of STI Statistics

- Site Test Interferometers (STI) have been operating at several sites over several year periods in order to acquire statistics on atmospheric turbulence effects applicable to uplink arraying
- Such statistics are useful in site characterization or inter-comparisons as well as estimating atmospheric degradation for potential or existing arrays that may occupy the site.
- In order to assess link degradation, one must adjust the statistics for the condition of the desired link and array configuration.
- We have earlier validated the integrity of the statistics and/or the available adjustment models
  - Validation with independent co-located instrument (WVRs next to each STI element at Venus Goldstone site)
    - Morabito, D. D., L. R. D'Addario, S. Keihm, and S. Shambayati, "Comparison of Dual Water Vapor Radiometer Differenced Path Delay Fluctuations and Site Test Interferometer Phase Delay Fluctuations Over a Shared 250-Meter Baseline," IPN PR 42-188, pp. 1-21, February 15, 2012.
  - Validation of two independent STI's at Goldstone by adjusting one STI to the conditions of the other STI
    - Morabito, D. D., L. R. D'Addario, R. J. Acosta, and J. A. Nessel (2013), Tropospheric delay statistics measured by two site test interferometers at Goldstone, California, Radio Sci., 48, doi:10.1002/2013RS005268.
  - Previous downlink array demonstrations involving the Cassini Spacecraft
    - Morabito, D. D., L. D'Addario, and S. Finley (2016), A comparison of atmospheric effects on differential phase for a two-element antenna array and nearby site test interferometer, Radio Sci., 51, doi:10.1002/2015RS005763.
- As a way of further testing the integrity of the accumulated statistics as well as the performance of the adjustment models, we conducted several additional downlink arraying demonstrations using arrays by tracking the Kepler spacecraft at the STI sites at Goldstone and Madrid.

Adjustments to STI Phase

$$\phi'_{array}(t) = \phi_{sti}(t)\,\frac{f_{array}}{f_{sti}}\left(\frac{\sin(\theta_{sti})}{\sin\left(\theta_{array}(t)\right)}\right)^{\gamma}\left(\frac{r_{array}(t)}{r_{sti}}\right)^{\beta/2}$$

f_{sti}, θ_{sti}, and r_{sti}, are the measurement frequency, elevation angle, and projected baseline length against STI signal source, respectively, of the STI instrument

f_{array}, θ_{array}, and r_{array}, are the measurement frequency, elevation angle, and projected array baseline length against the array signal source (Kepler spacecraft), respectively, of the DSN array

γ, and β are turbulence model dependent parameters later

- $r_{array}(t)$ and $\theta_{array}(t)$ are evaluated at each t using trajectory information.
- A static value of f_{array} = 32.166 GHz is used for the spacecraft frequency
- The value of r_{sti} represents the primary baseline of the data used in this study, (designated as baseline 1).

STI Values used for adjustments

Case	fsti, (GHz)	θsti, (deg)	rsti (m)
Goldstone Baseline 1	12.45	47.03	191
Madrid Baseline 1	11.95	41.32	163

Comparison of Array Phase and Adjusted STI Phase

- For array pass conducted on 2015-361 (December 27, 2015) involving Goldstone 34 m diameter antennas designated DSS-25 and DSS-26, we examined one hour periods
- The STI data over same period were processed to extract interferometer phase over all three baselines and adjusted to conditions of the Kepler array
- The resulting phase residuals from the 25/26 array (red) and adjusted STI phase (black) are shown in top panel for two successive time periods 02:00 – 03:00 UTC, and 03:00 – 04:00 UTC.
- As can be seen in the respective plots in the bottom panel, the cumulative distribution of the array phase (red) agrees quite well with that of the adjusted STI phase (black).

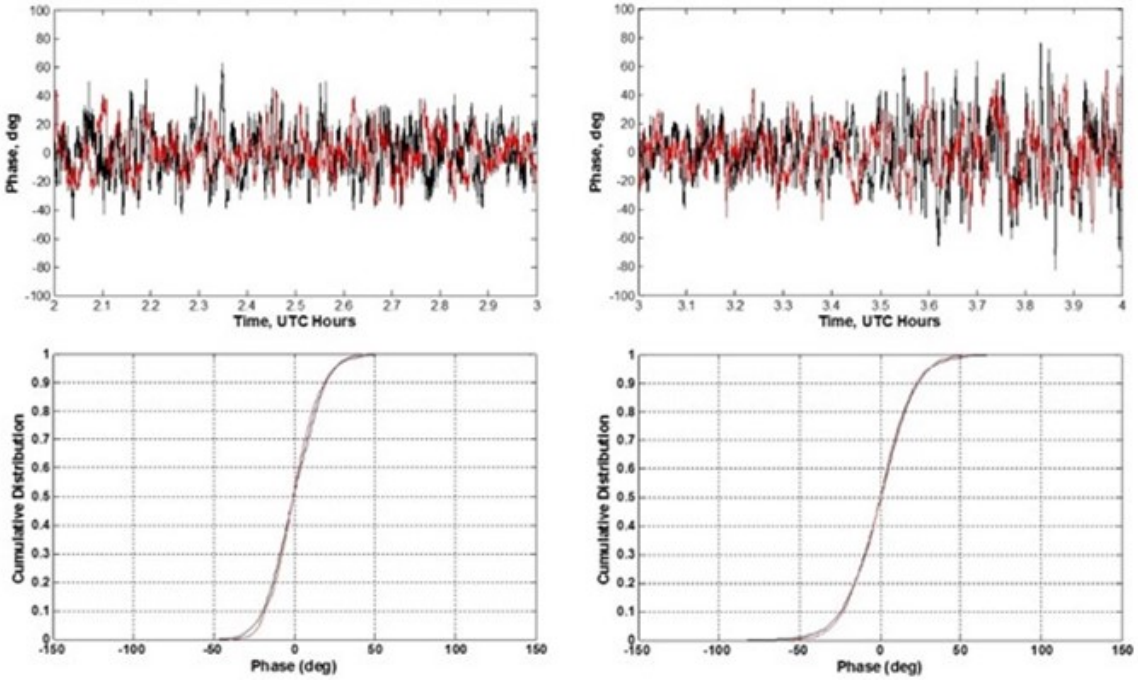

Goldstone DSS-25/DSS-26 Track on October 1, 2015

- By examining the phase time series over shorter time periods, we can better discern detail between the array phase and adjusted STI phase.
- Figure below displays the phase time series for one of these 10-minute time periods where the array phases are denoted by red and the adjusted STI phase time series in black
- There are periods of high correlation as well as with less correlation (or even anti-correlation or delays).
- There are comparable levels of fluctuations between the phases of the two instruments based on examination of the respective cumulative distributions for these data sets
- The Kepler signal path in the sky as seen by 25/26 array is near alignment with (within a few degrees) of the STI geostationary satellite signal path (STI azimuth = 201° elevation = 47°).

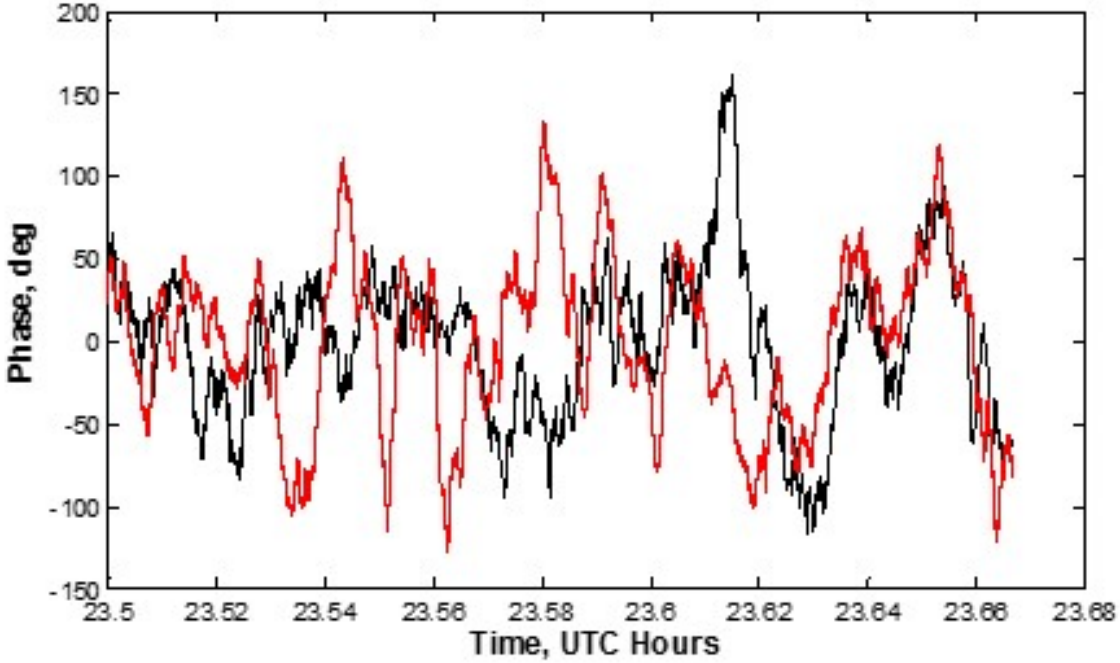

Overview of Array Demo Results

- If we calculate RMS scatter of the phase time series over 10-minutes intervals, we can compare the array and adjusted STI phase scatter.
- Data points for 2015-192 (25/26) (purple), 2015/361 (25/26) (red) and 2015-361 (54/55) (blue) lie close to or are reasonably distributed about the ideal curve.
- However, for pass 2015-274 (25/26) (yellow), almost all of the points lie above the ideal curve, suggesting that the array phase tends to exhibit more fluctuation than the adjusted STI phase. During this pass, the array was tracking Kepler at low elevation angles (~20° to 30°) compared to the location of the geostationary satellite observed by the STI (47°), thus we may be seeing more (non-isotropic) turbulence along the array signal path.
- One does not expect ideal or symmetric behavior as the atmosphere does not necessarily behave the same in all directions and signal paths the array and STI are sampling different parts of local atmosphere.
- The cases involving the short baselines involve adjustments based on the thick layer model as the lengths of both the STI baseline (~ 200 m) and DSN arrays (~ 300 m) are much smaller than the heights of the turbulent layer.
- The case of the longer 12.5 km baseline DSS-13/DSS-25 (2014-316/317) used an alternate adjustment scheme (filled green circles)

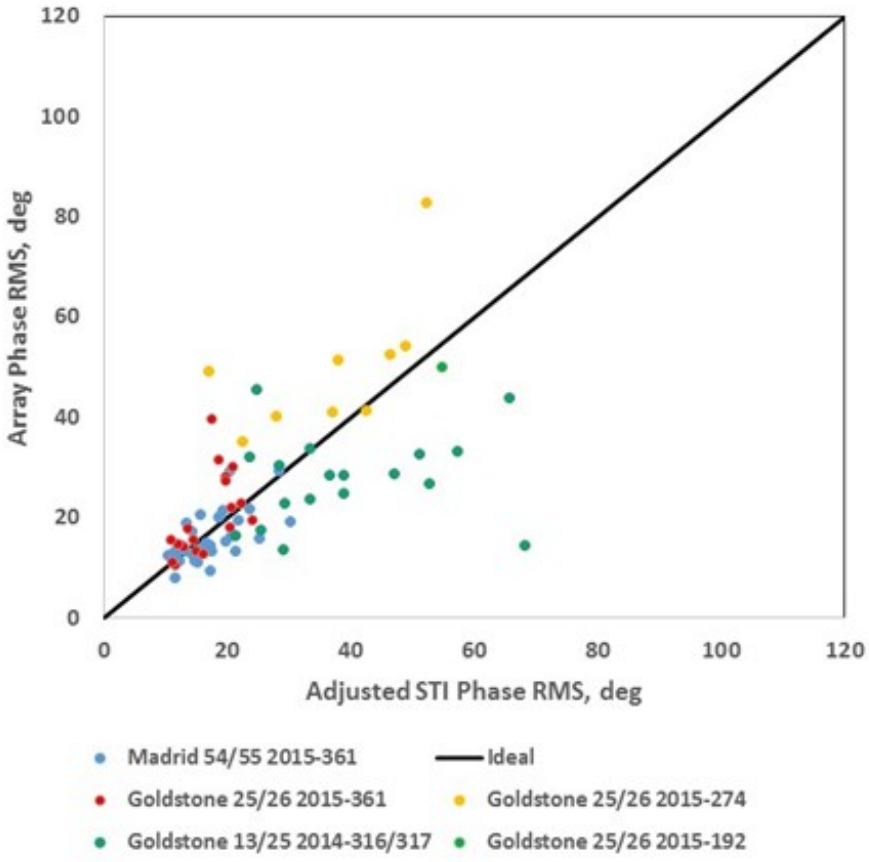

Madrid Array Demonstration on December 27, 2015

- Array demonstration of December 27, 2015 (2015-361) was performed using two Ka-band downlink capable 34 m antennas DSS-54 and DSS-55.
- Elements 2 and 3 of one of the STI baselines are located next to DSS-54 and DSS-55, respectively.
- The line-of-sight of the Kepler spacecraft as viewed by the 54/55 array is only ~1° from line-of-sight of the geostationary satellite as viewed by the STI for a portion of this pass.
- There is a very high degree of correlation between this STI baseline's adjusted phase time series (black) and the 54/55 array phase time series (red)
- The cumulative distribution for each of the two phase time series lie on top of each other.
- This is a significant result as it provides additional evidence that the models used in the adjustments are valid.

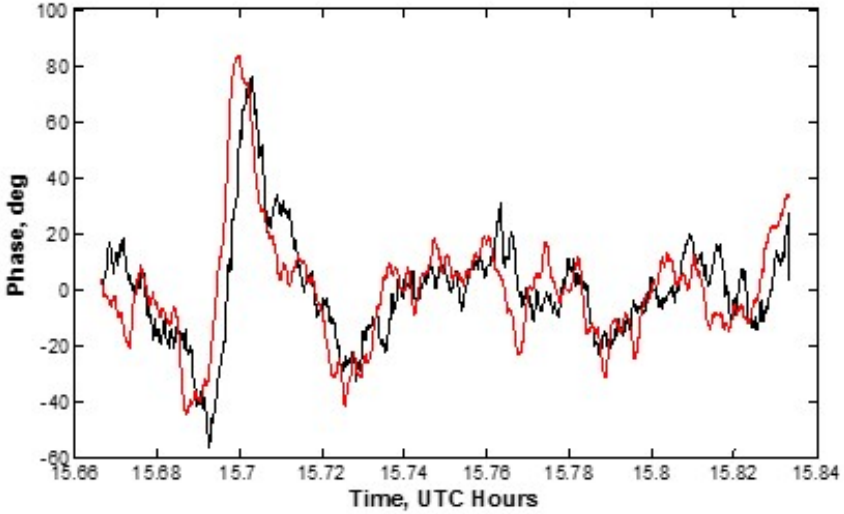

Madrid Array/STI Comparison Synopsis

- Slow features match well between the two instruments!
  - These correspond to large-scale irregularities in th turbulent flow moving across the antennas with the wind aloft
- Fast features do not match as well as the slow ones!
  - Fast features correspond to smaller scale irregularities in turbulent flow
- STI antennas, although adjacent to the DSN antennas, are not coincident as they are separated by ~ 21-35-m
  - When looking in the same direction, the signal paths are parallel but separated by that same distance
- The two instruments see the same large scale features but different small scale features
- The several second delays inferred from the data are consistent with the element separations and the range of wind speeds/directions obtained from the surface met data

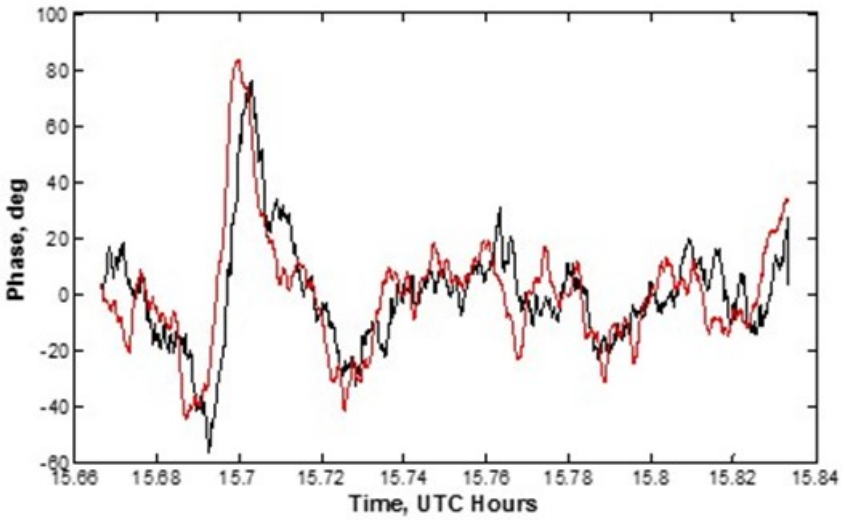

Conclusions

- Site Test Interferometers (STI) have been operating at several sites over several year periods in order to acquire statistics on atmospheric turbulence effects applicable to uplink arraying
  - Such statistics are useful in site characterizations, site inter-comparisons as well as estimating atmospheric degradation for potential or existing arrays that may occupy the site.
- In order to assess link degradation, one must adjust the statistics for the condition of the desired link and array configuration. Thus adjustments must be made for elevation angle, element separations, height differences and frequency differences using available models/assumptions.
- As a way of testing the integrity of the accumulated statistics as well as the performance of the adjustment models, we conducted several downlink arraying demonstrations using arrays tracking interplanetary spacecraft occupying the same site as the STIs for Goldstone and Madrid.
  - An earlier study using the Cassini spacecraft was published elsewhere.
  - The current study involved analysis of data from several passes involving the Kepler spacecraft.
- We found that the adjusted STI phase statistics over 10 min intervals were basically in reasonable agreement with those of the array even when the signal paths lie in different directions in the sky.
- For the case where the two signal path were co-aligned (within ~1 deg), we obtained excellent agreement in the phase signatures between the two data sets.

- Acknowledgements: We thank Danny Kahan of the radio science support team for his assistance in preparing and delivering the open-loop receiver data sets used in this study; DSN operations and the Kepler project for their cooperation. The research was carried out at the Jet Propulsion Laboratory, California Institute of Technology, under a contract with the National Aeronautics and Space Administration.

BACKUP

Tropospheric Assumptions

- We assume the troposphere is non-dispersive, thus the frequency adjustment is a simple scaling. Fluctuations caused by the ionosphere lie well below those of the troposphere
- The observed fluctuations will decrease with increase in elevation angle, θ, as air mass is inversely proportional to $\sin(\theta)$.
  - This dependence is linear ($\gamma = 1$) if turbulence along signal path is dominated by few large inhomogeneities.
  - If the turbulence is dominated by many small, random inhomogeneities, then their number along signal path is proportional to air mass, and effect on phase is proportional to the square root of that number ($\gamma = 1/2$)
  - The general case lies between these two cases and has a complicated dependence on the geometry, which involves the thickness of the turbulent layer, Hw, as well as the average distance between the two signal paths, r, whereas the latter depends on the baseline length r as well as the azimuth and elevation angles of the signal paths.
  - In most cases, the signal path separation is taken to be the projected baseline length perpendicular to the signal path direction (r ~ 100 to 200 m). The height of the turbulent layer is typically 1 to 2 km, so usually $r \ll Hw$, which leads to $\gamma \approx ½$.
  - In some cases Hw will be lower and γ will approach unity. For most analyses, we use $\gamma = ½$ for the thick screen model and $\gamma = 1$ for the thin screen model.
- The adjustment for baseline length r depends on the three-dimensional spatial structure function of the refractive index. Using the Kolmogorov theory of turbulence and integrating vertically through the turbulent layer gives the power law dependence with $\beta = 5/3$ when $r \ll Hw$ (thick screen) and $\beta = 2/3$ when $r \gg Hw$ (thin screen).
  - For this study, we used $\beta = 5/3$ for the thick screen model. In some cases, we used values derived from structure function fits of the STI data over the concurrent time interval of the array passes.